D2.4 Testing of large scale carbon fibre structures

[Version 1.0]

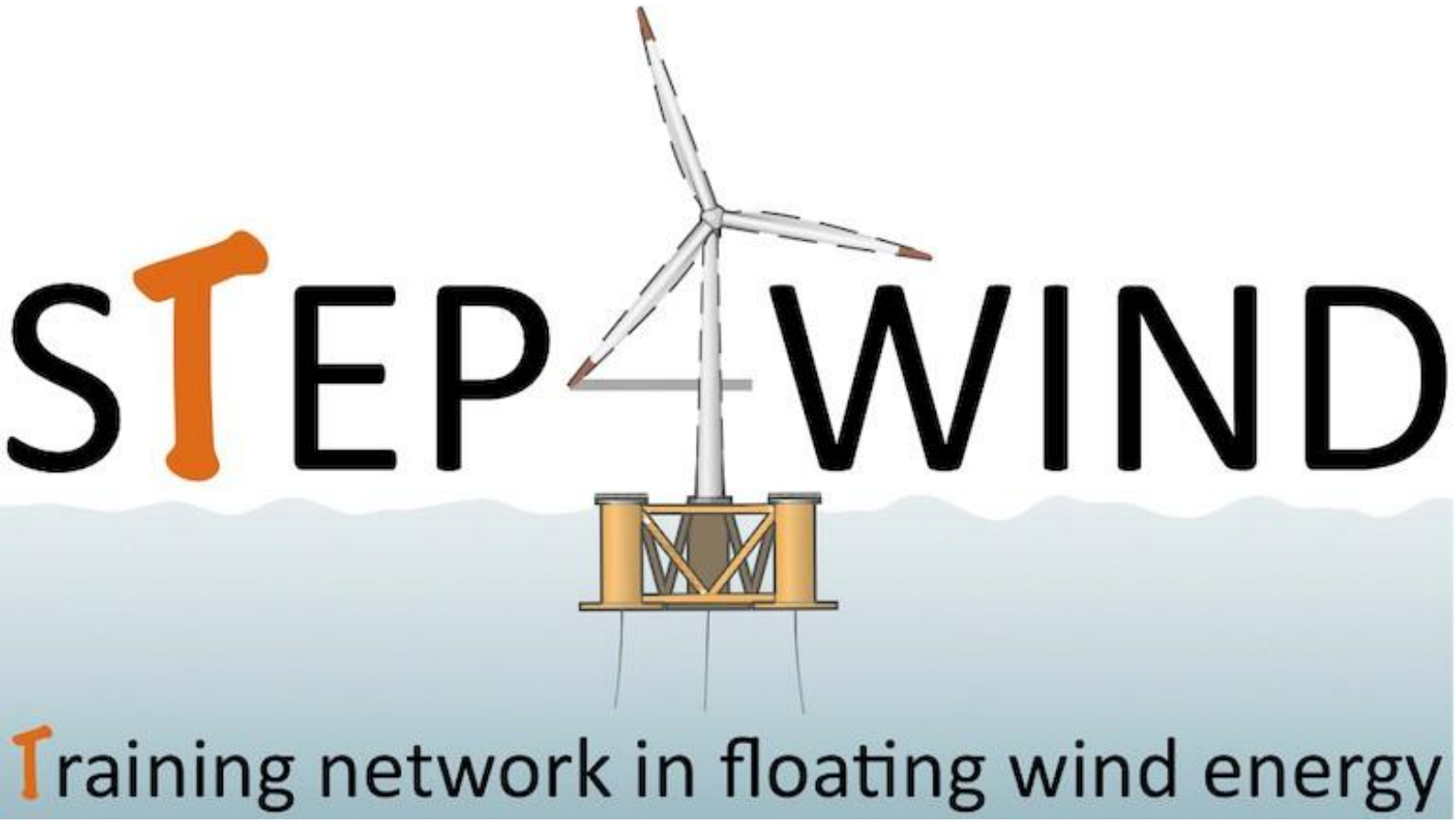

This project has received funding from the European Union's Horizon 2020 research and innovation programme under grant agreement No. 860737.

Document History

Revision Nr	Description	Author	Review	Date
1	First draft	Alejandro Jimenez del Toro (ESR 6)		July, 24th 2024
2	Final version	Alejandro Jimenez del Toro (ESR 6)	Oana Trifan	August, 16th 2024

Index

Disclaimer

Both D2.3 and D2.4 are to be seen in close relation to each other describing the experiments that have been conducted on the carbon-fibre thermoplastic composite parts. Both reports form the basis of the thesis of ESR6 on the novel manufacturing solution of wind turbine blades and automation.

This deliverable report D2.4 (Testing of large scale carbon fibre structures), is respectively reflected in the scientific publication entitled: ***The role of Ply orientation on the Resin flow under compaction in thermoplastic composites (****See Appendix). The title however, has changed due to the last year's developments in the field, thus a most proper way of defining the topic has been agreed, namely:* ***LAFP process optimisation for quality improvement and robust part production.***

Deliverable report, D2.3, is reflected in the journal publication entitled: ***The role of melting on intimate contact development in laser-assisted tape placement of carbon fibre reinforced thermoplastic composites*** *(Appendix of D2.3).*

1. Introduction

1.1. Context and background of the research question

Off shore floating wind energy has the potential to unlock green energy production for all costal countries in the European Union. Such technology makes use of floating wind turbines that can be deployed in deep waters, anchored to the sea bed by means of mooring lines. Compared to land based, i.e. on shore, wind farms, the levelized cost of energy are significantly higher for off shore farms, as the deployment, maintenance and decommissioning are more challenging. Thus, it is paramount to improve the productivity of off shore wind farms. Besides wind farm optimisation, increasing the rotor diameter of the wind turbines improves power output of the turbines. Hence, more power can be obtained from the same number of turbines, or less turbines are required to provide a certain power. This has led to an increase in the rotor dimensions over the recent years, resulting in wind turbine blades of above 100 meters long. To achieve such dimensions while maintaining the structural integrity, the thickness of the load bearing components in the turbine blades must be increased. Consequently, the lengthening of the blades results in an increase in their weight not only because of the extra length, but also because of the needed extra reinforcement. The weight increase is of major significance for any structure, even more a floating one, as it would negatively impact the design of the foundation plus the transportation, installation and decommissioning of the turbines and farms. Thus, reducing the weight while maintaining their mechanical performance is an important challenge for large blades.

An already adopted solution is to manufacture the blades with fibre reinforced composites. These materials consist of continuous fibres embedded in a polymer matrix. The fibres are the main load bearing components in the material, while the polymeric matrix holds the fibres together, transfers the loads between the fibres and bears the shear and out-of-plane loads. These composites have high specific mechanical properties, which means that their mechanical performance is high compared to their low density. Traditionally, wind blades have made use of glass fibre composites. And, although such fibres do allow to build large blades, their relatively low stiffness under tension imposes the need to significantly increase the thickness of the load bearing components in the blade, such as the spar caps. Alternatively, carbon fibre composites can be used to mitigate the weight increase due to the lack of stiffness of the glass fibres. Carbon fibres are significantly stiffer and even have a lower density. This leads to lighter blades than still can meet the performance requirements.

However, carbon fibre composites have their own drawbacks. Performance wise, it is acknowledged that their compressive behaviour can be poorer than that of glass fibre composites. This is due to the presence of instabilities at the microscale, caused by fibre misalignment, that leads to micro-buckling and the failure of the composite when loaded in compression. This can lower the compressive strength of the carbon fibre composites below the glass fibre ones. To mitigate such phenomena, a precise and accurate alignment of the fibre with the load direction is required. This is especially important in large blades. For instance, a misalignment of 0.5° in the fibre angle along a 100 m blade would cause a fibre deviation of 0.9 m; if the misalignment were 1°, the deviation would be of 1.7 m. Such potential misalignments imply that the blade would need to be designed with increased safety factors, which, in turn, would result in a further increase in the thickness of the parts. Thus, achieving a robust, precise and accurate fibre alignment is crucial to guarantee that the performance of the material is maximize and the weight of the structure is minimised.

In the light of the aforementioned points, an additive manufacturing technology is studied for the manufacturing of wind turbine blade spar caps. The automated fibre placement (AFP) technology is currently used in aerospace to manufacture carbon fibre composite structures. The composite material for the AFP comes in the form of tapes with continuous unidirectional fibres embedded in the polymer. These tapes are laid up one on top of, and next to, each other until the part is finished. As a computer numerical control machine, AFP is capable of placing tapes with high precision over the required distances, ensuring an adequate fibre alignment. In addition, it can do so following multi-angular layups, which can accommodate more complex

part designs, targeted to minimise weight and reduce scrap material. An AFP consists of two main elements, the heating source and the compaction roller. The heating source provides the energy required to bring the material to its optimal processing temperature. The compaction roller applies pressure to the heated material so that a well consolidated part, with no gaps or voids inside, is produced. Several parameters are of interest in AFP manufacturing, such as processing temperature, compaction force or placement speed.

Furthermore, AFP has the potential to produce the parts in a single step, without further postprocessing, when combined with carbon fibre reinforced thermoplastic composites. This is due to the so called in-situ consolidation capabilities of these thermoplastic matrices. Thermoplastic polymers are viscoelastic materials that consist of long, linear polymer chains. These chains are held together by entanglements, which are topological constraints that prevent them from flowing. These entanglements are reversible, weak interactions, which formation depends on temperature. Below a certain temperature, called the glass transition temperature, the entanglements are stable and the material has a more elastic-like behaviour, it cannot easily flow. Above such temperatures, the entanglements disappear and the material becomes more viscous, easing its flowability under pressure, and can be processed. Two types of thermoplastics can be identified based on the microstructure below the glass transition temperature. If the polymer chains remain entangled in a random configuration, forming an amorphous bulk, the thermoplastics are classified as amorphous. On the contrary, if part of the polymer chains can find a structured alignment and rearrange themselves into crystalline regions, the thermoplastic is called semicrystalline. In the later, the polymer microstructure then consists of amorphous and crystalline regions. The crystalline regions are significantly more stable to temperature than the amorphous ones and, as such, display their own behaviour with it. The melting point, which is higher than the glass transition temperature, is the temperature above which the crystals melt and a fully molten polymer is achieved. The region between the melting point and the glass transition temperature is where crystallisation occurs. The crystalline regions confer the thermoplastic and the composite mechanical and chemical properties that are of major interest for composite structures. Hence, only semicrystalline polymers are discussed below.

To achieve *in-situ* consolidation in AFP, two phenomena shall occur during compaction. First, the polymer matrix from the tape and the substrate must be brought together, into intimate contact, as it is called. Only then, the interdiffusion between the polymer chains across the interface can occur and the bulk properties restored. Unfortunately, in-situ consolidation only takes place when operating the AFP at very low rates, which are of no use for the wind energy industry. It has been estimated that intimate contact development is the rate controlling step in in-situ consolidation. This is due to the low viscosity of the thermoplastic matrices and low permeability of the fibre bed. The permeability of the fibre bed is a function of the fibre diameter and the fibre volume fraction (FVF) of the composite. The small fibre diameter of carbon fibre, of approximately 7 μm, and relatively high FVF of structural composites, between 55% and 60%, significantly hinder the flow ability of the material. However, these constrains are necessary to ensure the mechanical performance of the composite parts. Thus, it is the viscosity of the polymer what can be further considered to improve the intimate contact development in AFP.

The viscosity of a material refers to its ease to flow under shear stresses. As semi-crystalline thermoplastic polymers are made of long, entangled polymer chains, which are partially crystallised; their flowability is highly dependent on the length of these chains, i.e. polymer molecular weight, and the stability of these entanglements and crystals. A higher molecular weight usually delivers higher mechanical properties and lower viscosity, while a lower molecular weight polymer does the opposite. A compromise between mechanical performance and processability must be achieved when choosing the right polymer molecular weight for the intended application. For a given polymer molecular weight, it is both the temperature and the degree of crystallinity which has the greatest impact on viscosity for a semicrystalline thermoplastic. The role of processing temperature on intimate contact development has been extensively studied in literature, typically in combination with compaction pressure and placement speed. However, the role of crystallinity on intimate contact development has not been explored.

It is well known that crystallinity has a major impact on the viscosity. The presence of crystals increases the viscosity of the system to that of an elastic solid, hindering any flow. Crystallisation and melting refer to the formation and destruction of the crystals, respectively. These phenomena are mainly controlled by temperature, the temperature's rate of change and the reinforcement. In crystallisation, upon cooling down below the melting temperature and above the glass transition temperature of the polymer, crystallisation will start at a rate that is controlled by the mobility of the polymer chains which, in turn, is a function of temperature. At temperatures close the melting point, the crystallisation is very slow as the polymer chains have an elevated kinetic energy and is not favourable to arrange themselves into crystals. At temperatures close the glass transition temperature, the chains do not have enough kinetic energy, which prevents the necessary molecular movements to form the now more favourable crystals. A crystallisation optimum is found between these two temperatures. In turn, slower cooling and heating rates allow more time for crystallisation, enhancing it; while sufficiently high heating and cooling rates would hinder it. The role of the reinforcement in the crystallisation is complex and out of the scope of this thesis, therefore it will not be discussed further.

As AFP imposes complex temperature profiles during manufacturing, the formation and disappearance of the crystallinity in the composite could have a significant impact on its flowability and therefore in the intimate contact development. Thus, characterising the evolution of crystallinity throughout the AFP process is crucial to gain a deeper understanding of the technology and allow further optimisation towards achieving in-situ consolidation of composite parts.

1.2. Scope and outline of the thesis

In this thesis, it is chosen to explore the role that the phase transition kinetics of the thermoplastic matrix have on the intimate contact development of carbon fibre (CF) reinforced polyphenylene sulphide (PPS) composites (CF/PPS), manufactured by means of laser-assisted automated fibre placement.

In Chapter 2, the melting kinetics of PPS and CF/PPS are studied by means of fast scanning calorimetry (FSC). The phenomena of interest are: (1) the change in melting temperature of isothermal and non-isothermal crystals with the heating rate; (2) the effect of temperature and time on the melt memory effect; and (3) the effect that the fibre reinforcement may have on the melting kinetics of the matrix. A melting kinetics model will be derived from the experimental data for both materials. The melting models will be incorporated into a melting and crystallisation model in Chapter 4.

In Chapter 3, the non-isothermal crystallisation kinetics of PPS and CF/PPS are studied by FSC and differential scanning calorimetry (DSC). The combination of both techniques allows to analyse the crystallisation kinetics in a wide range of heating and cooling rates. This will improve the representativity of the experimental data towards developing a crystallisation model at both rapid and slow cooling and heating rates. Both, melt and cold crystallisation are studied, to account for the effect of nucleation on the crystallisation kinetics. A parallel Velisaris-Seferis model is chosen to represent such phenomena, as it accounts for the simultaneous development of primary and secondary crystallisation of PPS. The crystallisation kinetics models will be incorporated into a melting and crystallisation kinetics model in Chapter 4.

In Chapter 4, the melting kinetics model (Chapter 2) and the crystallisation kinetics model Chapter 3) are combined into a holistic phase transition kinetics model for PPS and CF/PPS. The CF/PPS model is validated against experiments using a static laser and laser assisted tape placement equipment. Validation of the PPS model is not possible by means of laser heating, as PPS is transparent to the infrared laser available at our facilities.

In Chapter 5, the developed phase transition kinetics model is used to evaluate the influence of such kinetics on the intimate contact development of the thermoplastic composites . The temperature region of interest lays between the glass transition and

the melting point of the composite. An LAFP with a self-heated tool are used to generate the samples. Different heating and cooling rates, as well as processing temperatures and placement speeds, will be impose to the material. The crystallisation and melting upon heating and cooling will be modelled using the phase transition kinetics model described in Chapter 4. Such kinetics will be studied against the intimate contact developed in the placement process. The final degree of crystallinity is also measured by DSC and compared to the predicted value from the model, as a validation step. Surface and cross-sectional microscopy are used to characterise the degree of intimate contact.

1.3. STEP4WIND deliverables related to the thesis

In light of these trends and developments, this thesis is reflected in two deliverable reports, which respectively are being addressed in two scientific publications. These reports focus on the same topic and address the same matters as initially thought, however the structured process steps, thus writing process, vary from the initial defined structure.

- D2.3 Automated process and characterisation of the laminates;
- D2.4 Testing of large scale carbon fibre structures, better defined as: **LAFP process optimisation for quality improvement and robust part production**, considering the recent developments in the field (addressed in this document).

2. LAFP process optimisation for quality improvement and robust part production

2.1. Abstract

To assess the role of crystallinity on the flowability of the composites, it is relevant to develop a methodology that allows for the systematic study of the different matrix flow present in the compaction of thermoplastic composites. These flows are: squeeze flow, longitudinal percolation flow and transverse percolation flow. In the first one, both matrix and fibre flow together, widening of the composite under pressure. The percolation flows involve the matrix flow along the static fibres, longitudinal, or across them, transverse. These flows are influenced by compaction force, compaction time. In addition, research has suggested that the substrate orientation can influence the contribution of each flow. Given that the carbon fibres are inextensible, they can hindering squeeze flow when placed perpendicular to the widening direction. Thus, a novel methodology is implemented to isolate the each different matrix flow in composites and the effect of compaction force, compaction time and substrate orientation are tested.

The full conference paper can be found in the Appendix.

2.2. Objectives

In order to assess the effect of the process parameters on the flow development of thermoplastic composites, the main objectives of this work are:

- Develop and test a novel methodology to study the different flows of the thermoplastic materials under compaction.
- Assess the effect of compaction force, compaction time and substrate orientation on the flow development of CF/PPS

2.3. Conclusions

This worked explored a new methodology to isolate the different flows in thermoplastic composites. The main conclusions are:

- The methodology successfully allowed the distinction between longitudinal and transverse percolation, as well as squeeze flow.
- Both percolation and squeeze flow increased with increasing compaction force and time.
- The substrate played a major role of the development of longitudinal and percolation flow. A parallel disposition induced further development of squeeze flow, while a perpendicular one prevented it, as expected.
- The preferred percolation flow was found to be dependent on compaction force, time and substrate orientation.

Appendix

The Role Of Ply Orientation On The Resin Flow Under Compaction In Thermoplastic Composites

Jimenez del Toro, Alejandro; Teuwen, Julie J.E.

Publication date
2024

Document Version
Final published version

Published in
Proceedings of the 21st European Conference on Composite Materials

THE ROLE OF PLY ORIENTATION ON THE RESIN FLOW UNDER COMPACTION IN THERMOPLASTIC COMPOSITES

Alejandro Jimenez del Toro[1], Julie J. E. Teuwen[2]

[1,2]Department of Aerospace Structures and Materials, Delft University of Technology, Kluyverweg 1, Delft, 2629 HS, The Netherlands
[1]Email: a.jimenezdeltoro@tudelft.nl
[2]Email: j.j.e.teuwen@tudelft.nl

Keywords: thermoplastics, compaction, percolation flow, squeeze flow, ply orientation

Abstract
In this study, a gap filling methodology was used to evaluate the flow behaviour of carbon fibre reinforced polyphenylene sulphide (CF/PPS) tapes under various compaction conditions (force and time) and layups. At each side of the gap, a different layup was present: 0/0 and 0/90. It was observed that squeeze flow occurred under all compaction forces and times, increasing with them. The layup influenced the squeeze flow development significantly, particularly visible in the change of the 0° fibre angle of the substrate across the gap. This fibre angle increased from the 0/90 to the 0/0, as the latter showed more squeeze flow than the former due to the parallel layup. The change of fibre angle across the substrate's width was indicative of the extent of the squeeze flow along its width. The percolation flow increased with compaction force and time, and both longitudinal and transverse flow were found. Longitudinal flow was visible at larger compaction forces, whereas transverse flow was the only flow found at lower ones. The development of transverse over longitudinal percolation flow is influenced by the layup, the sample configuration and the squeeze flow.

1. Introduction

Rapid processability of carbon fibre reinforced thermoplastic composites relies on effectively consolidating the laminates in a limited period of time. Such consolidation requires the development of intimate contact between the plies, plus the healing of the interfaces. Intimate contact development involves the flow of the composite under pressure, which would bring the thermoplastic matrix at both sides of the interface into contact.

Two types of flow are present in continuous fibre thermoplastic composites under compaction, squeeze and percolation flow. These flows can remove the surface asperities present in tapes and flatten the interfaces between two tapes for intimate contact. Squeeze flow involves the flow of fibres and matrix together in the transverse direction, widening the composite tape. Squeeze flow is highly anisotropic due to the presence of inextensible fibres in the longitudinal direction, which prevent deformation. Percolation is the flow of resin in the longitudinal and transverse direction to the fibre bed. The fibre bed permeability plays a significant role in the development of this flow. Such permeability is limited in both longitudinal and transverse directions, being one order of magnitude lower in the later [1]. The compact packing of the fibres and their small diameter contribute to the increased tortuosity in this direction. Simultaneously, the fibres impose a large extensional viscosity on the molten thermoplastic along their length.

Intimate contact models, to predict extent of flow in TP tapes during processing, based solely on the squeeze flow under compaction have been proposed and widely used. Yet, Celik et al. [2] showed that squeeze flow based intimate contact models could not successfully predict the experimental degree of intimate contact in CF reinforced polyetheretherketone single tape experiments in AFP. The authors concluded that squeeze flow and percolation flow, in both longitudinal and transverse directions, were

present, filling matrix poor areas at the surface of the tape. Thus, studying the contribution of each flow mode to the total flow of composites under different compaction conditions can lead towards further understanding the development of intimate contact.

In addition to the influence of the fibre orientation on the flow development within a tape, the orientation of the substrate on which it is placed can play a significant role too. It has been shown that substrate orientation can alter the squeeze flow behaviour in cross-ply layups [3]. The presence of inextensible fibres in different directions hinders the squeeze flow development of the whole layup. In doing so, percolation could then be promoted and found to be a greater contributor to the overall composite deformation [4]. Given the layup design flexibility in AFP, analysing the effect of the relative orientation between tape and substrate on the flow development is of relevance.

Mostly indirect methods of evaluating the different flow modes have been considered in literature so far. Kermani et al. [5] and Simacek et al. [6] developed a methodology to study the contribution of squeeze and transverse percolation flow in the gap filling process of composites. Their sample was a 0°/90°/0° cross-ply laminate made of unidirectional, continuous carbon fibre reinforced thermoset prepreg. The middle layer consisted of 90° plies with predefined gaps between them. The samples were compacted in an autoclave and the gap filling process was characterised by cross-sectional optical microscopy. The squeezed and percolated regions were visible, quantified. Their experimental results showed that percolation was the main contributor to the gap filling process and predicted a positive correlation between the increase in fibre bed permeability and the reduction of sample's thickness to the increase in transverse percolation flow.

The aim of this paper is to study the different flow modes during consolidation of thermoplastic composites for different ply orientations and compaction settings. Therefore, the setup described in [5,6] was adapted to, on top of squeeze flow and transverse percolation, also capture percolation in the longitudinal direction and the effect of ply orientation. We studied the behaviour of carbon fibre polyphenylene sulphide (CF/PSS) tapes in (0/0) and (0/90) orientation in a gap filling process performed in a dynamic-mechanical analyser (DMA) at different compaction forces and times. Optical microscopy was used to analyse the flow modes and to measure the resulting fibre angles due to squeeze flow.

2. Materials and Methods

The material used in this study is CF/PPS unidirectional tapes (Suprem®) with a fibre volume fraction of 55%. The tape's thickness and width are 0.15 mm and 6.35 mm, respectively. The nominal melting point of the resin is 280 °C, as measured by differential scanning calorimetry.

The specimen comprises two layers made with three tapes in total. Each tape is 6.35 mm wide, 0.15 mm thick and approximately 2 cm long. The substrate consists of one unidirectional tape oriented at 0°. The second layer consists of two tapes separated by a gap of 0.6 mm width and 6.35 mm length. One of the tapes is placed at a 0° orientation and the other at 90°. A small gap width was chosen to prevent or minimise protrusion of the substrate into the gap. Local compaction on the gap area is applied by an aluminium metal plate of 10 mm in width and 14 mm in length. This also allows to reach larger compaction pressures on the sample, as the DMA used is limited to 30 N of force. This generates a compaction width of 4.5 mm on each tape, and a total compaction area of roughly 60 mm^2. A representation of the sample layout and compaction area can be found in Figure 1a. Two fibre orientations are facing the gap, so that all three flow modes can contribute towards the gap filling process: squeeze flow and percolation flow in the transverse direction from the 90° tape (side A in Figure 1b), and longitudinal percolation from the 0° tape (side B in Figure 1b). In addition, the effect of the relative orientation between substrate and tape on the transverse squeeze and percolation behaviour can be assessed from the comparative analysis of sides A and C, as seen in Figure 1b, where side A represents a 0/90 layup and side C a 0/0 layup.

The samples are processed in a RSA G2 DMA (TA Instruments) with a 25 mm in diameter compression fixture. Between the metal plates and the composite, Kapton® tape is used to prevent them to stick. The

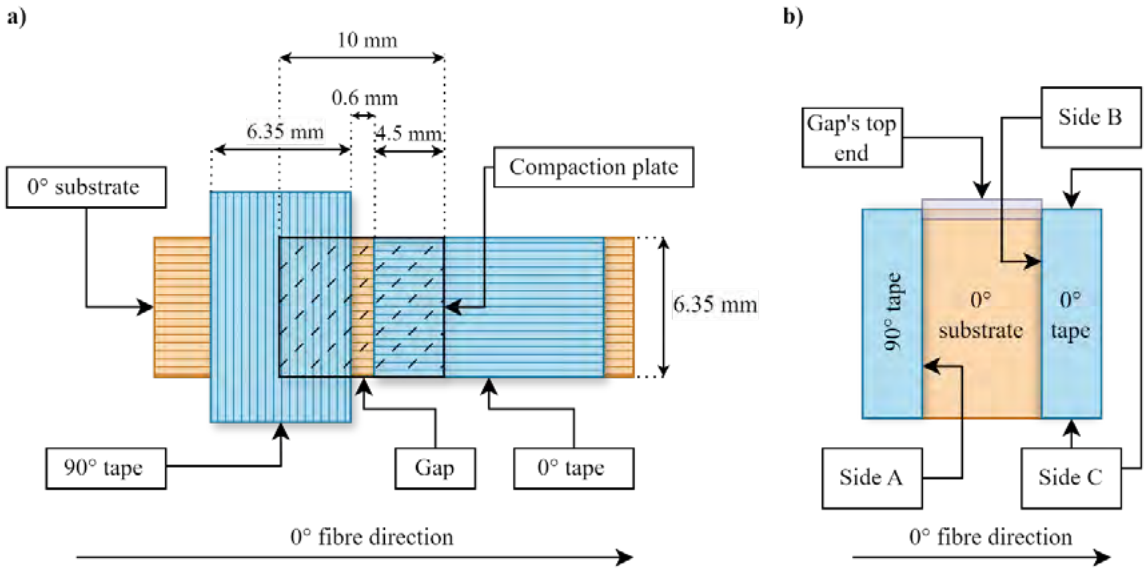

Figure 1. a) Schematics of the sample layout and the compaction area. The 3 CF/PPS ply arrangement including the gap between the two top tapes is shown. The compaction area is represented as a dashed area. b) Close up schematics of the gap area with the indication of the sides of interest (A, B, C, gap's top end) for the experiments

selected compaction forces, F_c, are 12 N and 24 N, which result in approximately 200 and 400 kPa of pressure, respectively. These forces are representative for AFP-like processing conditions. The tested compaction times , t_c, are 250 and 500 s. A force of 0.05 N and compaction time of 500s were used as a baseline. The different sample identifiers and their processing conditions can be found in Table 1. The samples are produced using an isothermal compaction program, so that the contribution of the temperature to the viscosity of the matrix is kept constant. At first, the temperature is increased from 40 to 360 °C at 10 °C/min, with a holding pressure of 0.05 N. The ramp is followed by an isothermal step at 360 °C, where the targeted compaction force, F_c, and time, t_c, are applied. At the end of this step, the sample is cooled down to 25 °C at 10 °C/min and a holding pressure of 0.05N is applied. The DMA program is represented in Figure 2.

The characterisation of the different flows in the sample is done by means of optical microscopy using a VK-X1000 confocal scanning microscope (Keyence®). The squeeze flow deformation of sides A and C is defined as the tape's maximum width increase with respect to the original tape's width. The original tape width is defined as the width of the tape that is not under the compaction plate. Note that, as there are two sides C, the final side C deformation reported is the average of both sides, so that it can be compared to side A. The effect of different layups on squeeze flow behaviour of the substrate is characterized by analysing the change of the substrate's fibre angle across the gap's width, as fibres transition from a 0/90 layup on side A to a 0/0 layup on side B. The resulting fibre angles observed in the substrate are calculated with respect to the original 0° fibre angle of the substrate and are evaluated along the gap's length, from the its top end, i.e. 0 µm, see Figure 1b, to approximately the middle line of the gap, i.e. 3000 µm. The other half of the gap is considered symmetrical. Only the visible fibres could be measured. As a significant degree of scatter in the fibre angle was found, the gap's length was divided in 200 µm sections. For each section, the average fibre angle and its standard deviation were estimated, when more than one fibre was identified. Finally, the extent of percolation flow was estimated by the ratio of the resin-covered gap length to the total gap length in the tested samples.

Table 1. Process conditions used in DMA for compaction force and time with their corresponding sample identification labels.

Sample ID	Compaction force, N	Compaction time, s
Reference	0.05	500
12A	12	250
12B		500
24A	24	250
24B		500

3. Results

The gap micrographs for all tested samples can be found in Figure 3. Firstly, the gap filling in terms of percolated resin will be presented. The isothermal compaction of the samples results in resin percolation within the gap when a force of 24 N is applied (Figure 3d and 3e). At longer compaction times (24B), the resin fills 83% of the gap's length while for shorter times (24A) it is 42%. The matrix front across the gap width is higher at side B (0/0) compared to side A (0/90) for longer compaction times (24B), while this is not visible in 24A, as both sides are equally covered. In addition, a matrix droplet can be seen on side A (0/90) for shorter compaction times (24A). Samples at lower compaction forces (12A and 12B) do not show gap filling, Figure 4b and 4c; yet, for longer compaction times (12B), droplets of matrix are spotted at side A (0/90). The reference sample, Figure 4a, does not display any percolated resin within the gap area. No percolated resin was found on side C (0/0) for any test configuration.

Secondly, squeeze flow is also observed after the experiments, on side C (squeeze flow of the 0/0 layer) and side A (squeeze flow of the 90 layer), see Figure 4 for maximum width increase observed at these locations. Squeeze flow is observed on side C at all forces and compaction times. The same holds for side A except for the reference case of 0.05 N force. The largest squeeze flow of side C is measured for the highest compaction force and time (24B) and it decreases with both. The effect of the compaction force is far more noticeable than that of time. A similar behaviour is found for side A (0/90), yet the percolated resin does not allow to accurately determine the squeezed front for the highest force (24A and 24B), thus no further analysis can be conducted on this.

Also a change in the original 0° fibre angle of the substrate is observed across the gap's width, as it is clearly visible in Figure 3e and 3d compared to 3a. Figure 5 shows the averaged fibre angle along approx. half of the gap's length as a function of the compaction conditions. The fibre angles reach a maximum value, θmax, close to the free edge and increase with both force and time under compaction. We observed a range of θmax from 4.5%-15.9% for the different compaction setting, see also Figure 4. After that, all samples, except for the reference, show an asymptotic decreasing trend towards the middle of the tape width, where the values converge to the angles of the reference sample (indicative values of their initial fibre angle of 0°). Note that the percolated resin in sample 24B does not allow to characterise the fibre angle beyond 800 μm. The distance over which the fibre angles decrease towards 0° also increases with the compaction force and time.

4. Discussion

4.1. Squeeze flow

The squeeze flow measured on side C of the tape increases with both force and time, as expected. The effect of the compaction force is more significant than that of the compaction time. A 3% increase in tape's width is seen between 250 and 500 s for both compaction forces, 12 and 24 N. Doubling the compaction force, from 12 to 24 N, induces a 5% increase on the tape's width for both compaction

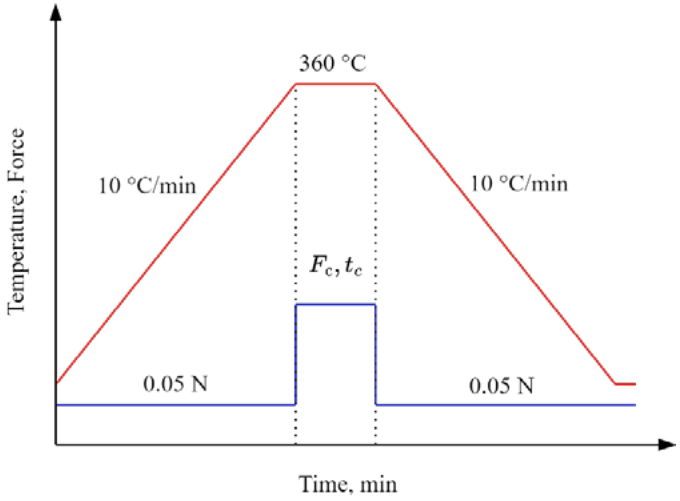

Figure 2. DMA temperature and force profile schematics. The values of the compaction force, F_c, and time, t_c, can be found in Table 1.

times. This can be related to the larger deformation rate achieved by applying larger compaction forces. The squeeze flow observed on side A is 1% lower than that of side C for the reference and 12A samples, while they are equal for 12B. The layup does not seem to play a significant role on the maximum width increase between sides A and C for the samples tested at 12 N.

On the substrate, the increase of fibre angle across the gap's width can be related to a more developed squeeze flow of the 0/0 layup compared to the 0/90 one. The perpendicular, inextensible fibres of the 0/90 layup constrain the squeeze flow of the substrate, maintaining the original 0° angle of the substrate's fibres, as observed in Figure 3d and 3e. On the contrary, the substrate is able to further develop squeeze flow on a 0/0 layup, due to the cooperative movement between two plies with parallel fibres. The displacement of fibres, along with the resin, in the transverse direction of the substrate generates a distortion of the fibre angle across the gap. As seen in Figure 4, the measured θmax increases with compaction force and time, as it would be expected for squeeze flow, and correlates well with the deformation of side C. The observed differences on the effect of the layup on the squeeze flow behaviour of the substrate and the tapes are not yet clear from these experiments.

The change in fibre angle with the distance to the gap end can be interpreted as the squeeze flow developing across the substrate's width. Figure 5 shows that the extent of the squeeze flow across the gap length is a function of both, the compaction force and time, with larger times and forces inducing larger affected areas. The fibres near to the edge of the gap are the most affected ones, registering a larger angle change. The closer to the middle line of the substrate, at approximately 3000 μm, the lesser the angle of the fibres, indicating a less developed squeeze flow across the substrate's width. As the squeeze flow induces a change in the fibre bed arrangement and therefore its permeability, this could affect the development of percolation flow across the substrate's width. Hence, the different flow modes could have a heterogeneous contribution to the intimate contact development across the width of the compacted tape.

4.2. Percolation flow

Percolation flow is found to contribute more towards the gap filling process with increasing compaction forces and times. Due to the limited tested compaction forces and times, there are not enough data points to track the evolution of the percolated matrix for all samples. Yet, two distinct percolation modes are found as a function of the compaction force after 500 s.

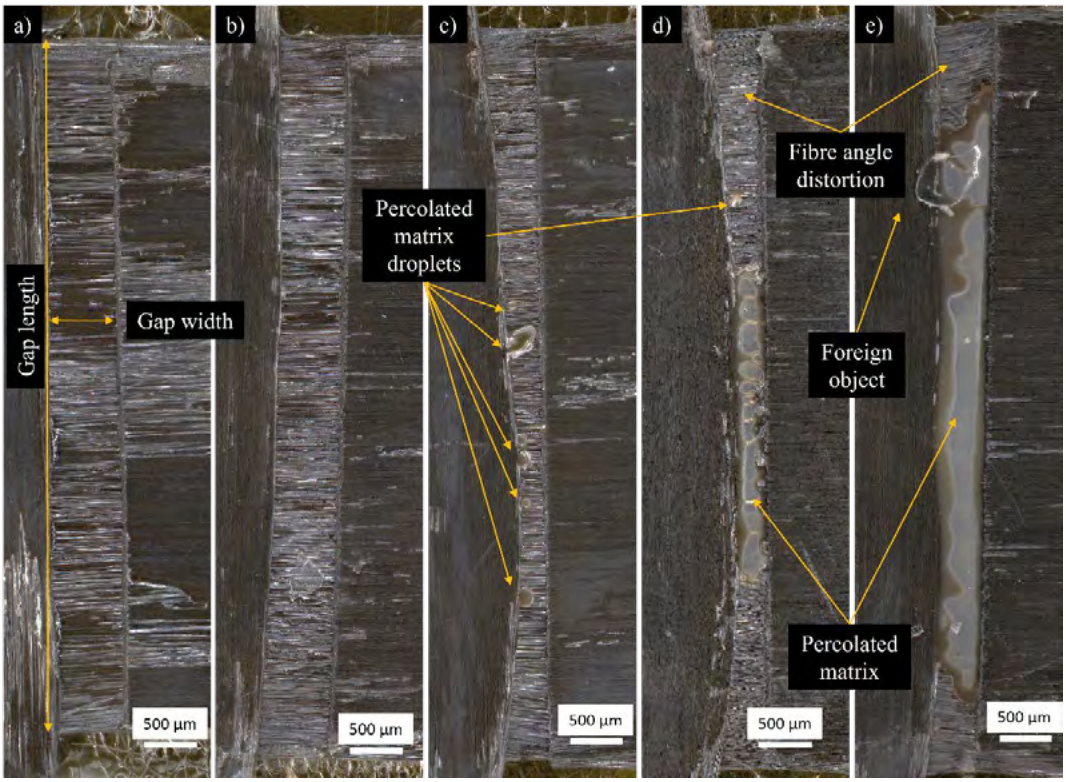

Figure 3. Gap micrographs for all tested samples (top view, showing sides A and B from Figure 2), for different compaction settings (see Table 1), as a) Reference, b) 12A, c) 12B, d) 24A and e) 24B. The magnification used for all micrographs is 12x. Features highlighted in the figures are gap length and width, in a); percolated matrix droplets, in c) and d); fibre angle distortion and percolated matrix in d) and e); foreign object in e).

A higher compaction force (24B) has a larger percolation contribution to the gap filling compared to a lower one (12B), which indicates a strong dependency of the percolation flow with the compaction force (Figure 4c and 4e). The greater coverage of resin on side B (0/0) compared to side A (0/90) in the gap area suggests that the resin front across the gap originated from side B, indicating that longitudinal percolation is present in 24B. The individual contribution of longitudinal and transverse percolation flow to the gap filling process of sample is not measurable from this characterisation. The lack of longitudinal percolation flow at a lower compaction force (12B) suggests a compaction force dependence on the preferred percolation mode.

At a lower compaction force (12B), the sample has matrix droplets throughout its side A (0/90), as seen in Figure 4c. These can be related to transverse percolation occurring upon these conditions. Yet, no longitudinal percolation is found on side B (0/0), which has a higher permeability and therefore should be preferred. Furthermore, no transverse percolation is found in side C either (0/0), which undergoes the same deformation upon compaction as side A. The lack of percolation flow on sides B and C can be attributed to the development of squeeze flow in both the substrate and the tape in the 0/0 layup. This would ease the localised pressure on both sides as it allows the widening and thinning of the 0/0 stack, hindering the development of any percolation flow. To the contrary, a higher localised pressure would be found on side A (0/90), as the cooperative squeeze flow of tape and substrate is not possible.

In addition, two more factors contribute towards the development of transverse percolation flow. First, both ends of the 90° tape extend beyond the compaction area, effectively blocking the more favourable longitudinal percolation flow. And, second, as side A undergoes squeeze flow upon compaction, the initial fibre bed permeability is altered, which can further contribute towards easing transverse

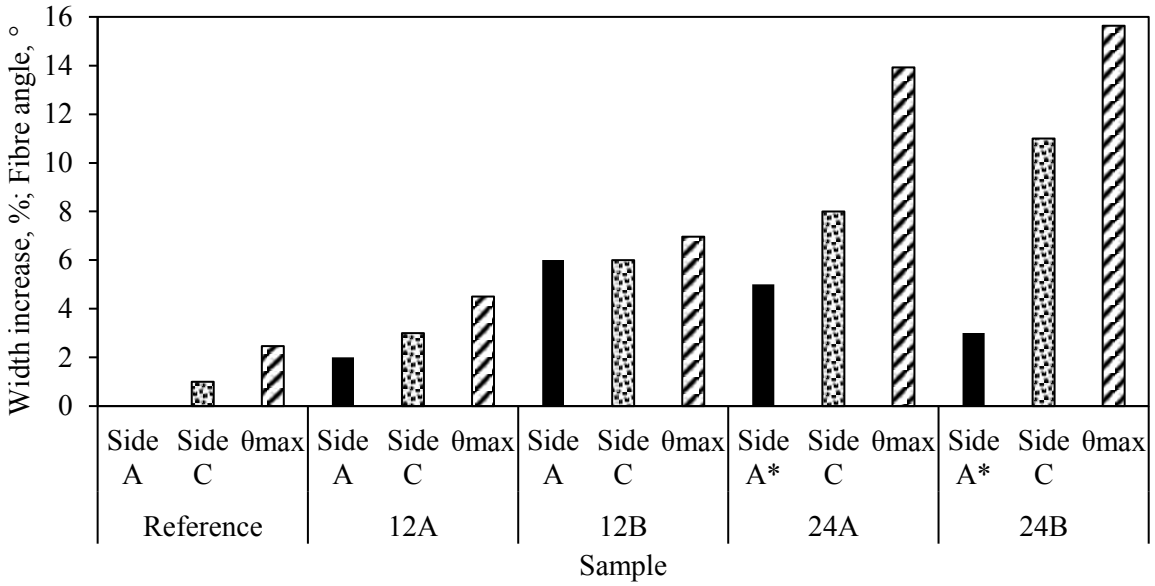

Figure 4. Results for the maximum width increase of sides A and C and the maximum fibre angle change within the gap area for all tested configurations. The * indicates not conclusive values.

percolation. The lesser squeeze flow found at lower compaction times (12A) would be responsible for the lack of transverse percolation in these conditions. Finally, it is also worth noting the lack of transverse percolation on side C at higher compaction forces (24B), which clearly indicates that compaction force and squeeze flow are not enough to promote transverse percolation over the more favourable squeeze and longitudinal percolation flows. Instead, the layup and the boundary conditions of the compacted area have a significant influence on the preferred percolation flow.

5. Conclusions

In this work, an experimental gap filling methodology was successfully applied on CF/PPS composites. It allowed to evaluate the different flow modes of the composite upon different compaction conditions and layups. At each side of the gap, a different layup was present: 0/90 and 0/0. Squeeze flow was found at all tested compaction forces and times, and was force and time dependent. The effect of the layup on the squeeze flow development was clearly seen in the change of the original 0° fibre angle of the substrate across the gap area. The 0/90 layup hindered the squeeze flow of the substrate due to the presence of inextensible fibres in the 90° direction, retaining more effectively its original width and therefore the 0° angle of the fibres. The 0/0 layup allowed the cooperative squeeze flow of substrate and tape, widening the substrate. The fibre displacement due to squeeze flow imposed a fibre angle change across the gap, which indicated the extent of the squeeze flow across the width of the substrate. The gradient in fibre angle can also be related to a gradient in the fibre bed permeability, which could impose a heterogenous flow behaviour across the width of the compacted tape.

The percolation flow was also found to increase with compaction force and time, yet the preferred flow mode was influenced by the layup and the boundary conditions around the compacted area. Longitudinal percolation flow was present at higher compaction forces, as the resin front in the gap developed from the 0° tape at the 0/0 layup. Transverse percolation was favoured at lower compaction forces from the 90° at the 0/90 layup, where no longitudinal flow was found. This is due to several factors: first, the increased localised pressure in the 0/90 layup due to the lack of squeeze flow of the substrate; second, the squeeze flow of the 90° tape increases the transverse permeability; and, third, both ends of the 90° extended outside the compacted area, blocking the longitudinal flow. Thus, the preferred percolation flow is a function not only of the compaction force and time, but also the layup

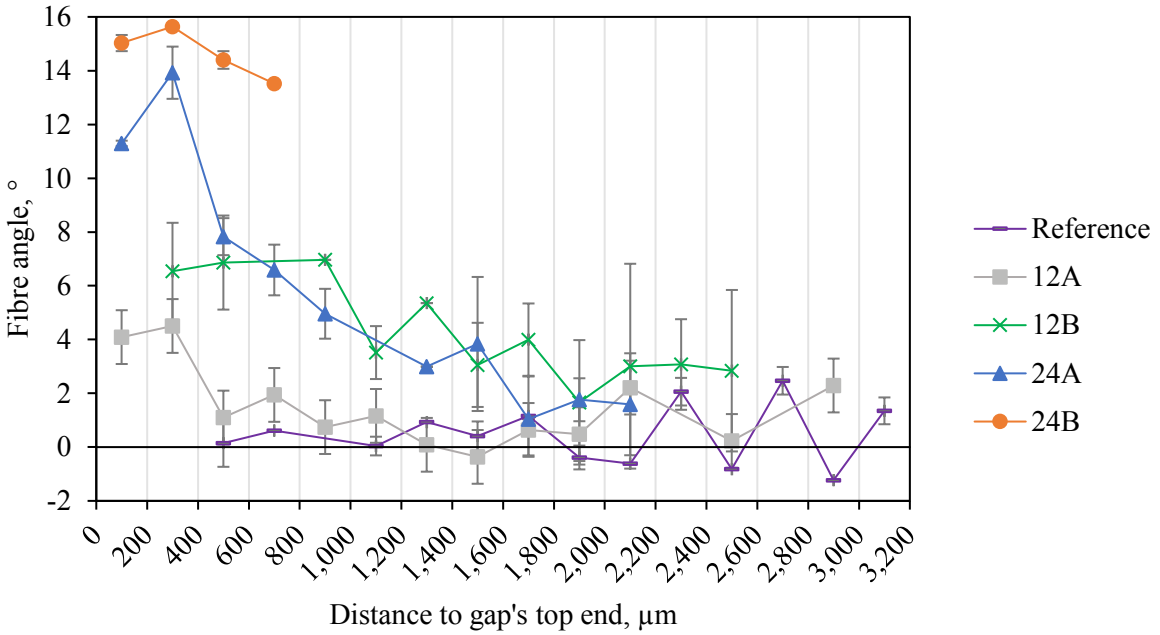

Figure 5. Evolution of averaged fibre angle along the gap's length at 200 µm intervals for each tested configuration.

and boundary conditions of the compacted area. These findings can help understand how the composite flow develops in AFP and convey strategies to improve intimate contact development.

Future work will include: (1) expanding these experiments to more compaction forces, times and layups in DMA as well as in AFP; (2) isolating each flow mode by having the same layup at both sides of the gap; and (3) using cross-sectional microscopy and micro-CT to determine the contribution of each flow mode to the gap filling process, as well as the role of fibre bed permeability on the transverse and longitudinal percolation.

References

[1] Amin, M, et al. "Longitudinal and Transverse Flows in Fiber Tows: Evaluation of Theoretical Permeability Models through Numerical Predictions and Experimental Measurements." Composites Part A: Applied Science and Manufacturing, vol. 119, 1 Apr. 2019, pp. 73–87, https://doi.org/10.1016/j.compositesa.2018.12.032.

[2] Çelik, Ozan, et al. "Intimate Contact Development during Laser Assisted Fiber Placement: Microstructure and Effect of Process Parameters." Composites Part A: Applied Science and Manufacturing, vol. 134, July 2020, p. 105888, https://doi.org/10.1016/j.compositesa.2020.105888.

[3] Kobler, Eva, et al. "Modeling the Anisotropic Squeeze Flow during Hot Press Consolidation of Thermoplastic Unidirectional Fiber-Reinforced Tapes." Journal of Thermoplastic Composite Materials, 20 Nov. 2023, https://doi.org/10.1177/08927057231214458.

[4] J.A. Goshawk, et al. "Squeezing Flow of Continuous Fibre-Reinforced Composites." Journal of Non-Newtonian Fluid Mechanics, vol. 73, no. 3, 1 Dec. 1997, pp. 327–342, https://doi.org/10.1016/s0377-0257(97)00049-9.

[5] Niknafs Kermani, Navid, et al. "Gap Filling Mechanisms during the Thin Ply Automated Tape Placement Process." Composites Part A: Applied Science and Manufacturing, vol. 147, Aug. 2021, p. 106454, https://doi.org/10.1016/j.compositesa.2021.106454.

[6] Simacek, Pavel, et al. "Role of Resin Percolation in Gap Filling Mechanisms during the Thin Ply Thermosetting Automated Tape Placement Process." Composites. Part A, Applied Science and Manufacturing, vol. 152, 1 Jan. 2022, pp. 106677–106677, https://doi.org/10.1016/j.compositesa.2021.106677.